Proteomic identification of CIB1 as a potential diagnostic factor in hepatocellular carcinoma

Tong Junrong[1,†,*], Zhou Huancheng[2,†], He Feng[1], Gao Yi[2], Yang Xiaoqin[3], Luo Zhengmao[1], Zhang Hong[1], Zeng Jianying[1], Wang Yin[1], Huang Yuanhang[1], Zhang Jianlin[1], Sun Longhua[1] and He Guolin[2]

[1]*Department of Nephrology, Guangzhou Army General Hospital Guangzhou 510010, China*

[2]*Department of Hepatobiliary Surgery, Zhujiang Hospital, Southern Medical University 510282, China*

[3]*Institute of Genetic Engineering, Southern Medical University 510515, China*

[†]*These authors contributed equally to this work.*

**Corresponding author (Fax, +86-02036653565; Email, tongjr63@163.com)*

Hepatocellular carcinoma (HCC), among the most common malignancies worldwide, remains a major threat to public health, and there is an urgent need to identify novel biomarkers for diagnosis, prognosis and targets for anti-cancer treatment. In this study, two-dimensional polyacrylamide gel electrophoresis coupled with ESI-Q-TOF MS/MS analysis was used to identify differentially expressed proteins among the HCC tumour centre, tumour margin and nontumourous liver tissues. In total, 52 spots with significant alteration were positively identified by MS/MS analysis. Altered expression of representative proteins, including CIB1, was validated by Western blotting. Immunostaining suggested an increase tendency of CIB1 expression from nontumourous liver tissue to tumour centre. Knockdown of CIB1 expression by RNA interference led to the significant suppression of the cell growth in hepatoma HepG2 cells. These data suggest that CIB1 may be used as a novel prognostic factor and possibly an attractive therapeutic target for HCC.

[Junrong T, Huancheng Z, Feng H, Yi G, Xiaoqin Y, Zhengmao L, Hong Z, Jianying Z, Yin W, Yuanhang H, Jianlin Z, Longhua S and Guolin H 2011 Proteomic identification of CIB1 as a potential diagnostic factor in hepatocellular carcinoma. *J. Biosci.* **36** 659–668] **DOI** 10.1007/s12038-011-9101-6

1. Introduction

Hepatocellular carcinoma (HCC) is among the most common malignancy in both underdeveloped and developing countries, leading to 600000 deaths annually worldwide (Farazi and DePinho 2006). HCC is especially frequent in Asia due to a high prevalence of chronic HBV and HCV infections (Raza *et al.* 2007). Lacking effective biomarkers, many patients diagnosed at the advanced stage miss the best opportunity for anti-cancer therapy, including liver resection or transplantation. Furthermore, the postoperative 5-year survival is relatively low at 30%–40%, since the patients who were resected often suffer a high frequency of tumour metastasis/recurrence (Hwang 2006). Hence, research into screening new HCC diagnostic biomarkers and alternative mechanisms of HCC carcinogenesis is still required.

As is the case with tumours in general, HCC is believed to develop following multi-pathogenetic steps, initially with pre-malignant lesions, through hyperplasia to dysplasia, then carcinoma *in situ*, and finally invasive carcinoma (El-Serag and Rudolph 2007). Previously, factors such as transforming growth factor (TGF-α), TGF-β, and p53 were well known to play important roles in hepatocarcinogenesis (Tseng *et al.* 2008; Wang *et al.* 2008). Recently, advances in genomic technologies have made it possible to rapidly screen for global and specific changes in gene expression that occur

Keywords. CIB1; 2-DE; hepatocellular carcinoma; proteomics; proliferation

Supplementary materials pertaining to this article are available on the *Journal of Biosciences* Website at *http://www.ias.ac.in/jbiosci/Sep2011/pp659–668/suppl.pdf*

only in cancer cells. Studies using DNA microarray-based approaches have identified a large body of transcriptional events, induced by various genetic and epigenetic modifications (Maass *et al.* 2010). However, these genetic changes cannot precisely reflect the biological nature of cancer cells or the clinical characteristics of individual HCC patients. Therefore, expression profile analysis at the protein level is an essential step for understanding the mechanisms of hepatocarcinogenesis and in discovering diagnostic markers and therapeutic targets for HCC.

Proteomics, a study of the complete protein complements of the cell, is a promising approach in the identification of proteins which may be used as new targets for therapeutic intervention and as markers for early detection of cancers (Cho 2007). In contrast to the genome, the proteome is dynamic and is in constant flux because of a combination of factors, such as differential splicing of the various mRNAs, post-translational modifications, and temporal and functional regulation of gene expression (Petricoin *et al.* 2002). To date, proteomic approaches have been extensively employed in studies of various tumours, including HCC (Wulfkuhle *et al.* 2003). By comparing the protein expression profiles between HCC and normal cell lines or tissues, replicable and significant changes, including glycolytic enzymes, transcriptional factors and serum proteins, have been obtained (Comunale *et al.* 2006; Sun *et al.* 2007). Nevertheless, the profiles from various reports were limited to a small group of proteins, and only very few of them have been functionally analysed for their roles in hepatoma cell. Furthermore, the alteration pattern of these proteins is not in chorus, reflecting their regional variability or tissue heterogeneity. Thus, a more detailed profiling is still needed to identify the unrevealed protein factors underlying the HCC carcinogenic process.

In the present study, we utilized a 2-DE-based proteomic approach to profile the altered expressed proteins among HCC tumour centre, tumour margin and nontumourous liver tissues from ten HCC patients. Of the 52 dysregulated proteins, we found and validated that CIB1 expression was gradually upregulated in tumour margin tissues and tumour centre tissues compared with nontumourous liver tissues. Further, functional analyses demonstrated that CIB1 is crucial for proliferation of hepatoma cell line. The data presented in this study suggested that CIB1 could be developed as a useful diagnostic biomarker, as well as a potential therapeutic target for hepatocellular carcinoma.

2. Results

2.1 *2-DE profiling of differentially expressed proteins in HCC*

The protein expression profiles among HCC tumour centre, tumour margin and nontumourous liver tissues were obtained by 2-DE. The detailed information of clinical samples used for 2-DE analysis is listed in supplementary table 1. Gel images and representative 2-DE maps were unambiguously matched by the PD-Quest software, and the representative 2-DE maps are shown in figure 1. Approximately 1500–1600 protein spots were detected by silver staining in a single 2-DE gel. The quantity of each spot in a gel was normalized as a percentage of the total quantity of all spots in the gel. Differentially expressed spots were defined by intensity alterations >2.0-fold ($P<0.05$) from any of the paired comparison (tumour centre and tumour margin, tumour centre and nontumourous liver tissue, or tumour margin and nontumourous liver tissue) in one sample group. Only those differentially expressed spots with recurrences of more than 6 times in the 10 groups of samples examined were subjected to MS/MS analysis. By applying these criteria, a total of 52 spots were identified.

2.2 *Mass-spectrum identification of differentially expressed proteins*

Differentially expressed protein spots were subsequently subjected to MS/MS analysis. The MS/MS data were retrieved using the search algorithm MASCOT against the Expasy protein sequence database. The proteins were identified using a number of criteria including MW, the number of matched-peptides and ions score. Only those proteins with a score >38 ($P<0.05$) were selected and listed in the table 1.

2.3 *Bioinformatics analysis of the identified proteins*

We used the Web-based tool Batch Query (*http://pid.nci.nih.gov/search/batch_query.shtml*) and Toppgene (*http://toppgene.cchmc.org/ToppGene/network_prioritization.jsp*) to analyse the biological processes associated with the identified proteins. We applied ToppGene independently to the up- and downregulated proteins. As results, 29 different signaling pathways ($P<0.05$) were obtained, including hemopoietic progenitor cell differentiation, anatomical structure formation involved, T cell activation etc. (supplementary figures 2–3). The extension of these signallings to other proteins could be useful to advance in the knowledge of the formation and progression of HCC.

2.4 *Validation of the altered proteins in HCC*

To examine whether the proteomics identification of altered proteins corresponding to the changes at the translational level, six proteins (CIB1, STMN1, Gankyrin, PRDX6, 14-3-3, ARIH1) with significant expression changes were chosen for

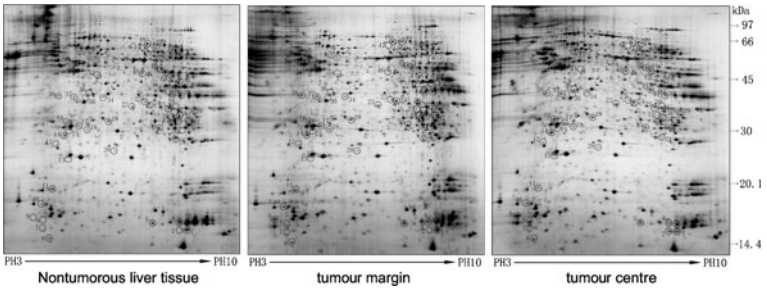

Figure 1. Representative 2-D gel images of HCC tumour centre, tumour margin and nontumourous liver tissues. Total protein extracts were separated on pH 3–10 nonlinear IPG strips in the first dimension followed by 12% SDS-PAGE in the second dimension and visualized by silver staining. Approximately 1500–1600 protein spots were detected by silver staining in a single 2-DE gel. The quantity of each spot in a gel was normalized as a percentage of the total quantity of all spots in the gel. A total of 52 spots were identified.

validation by Western blot. As shown in figure 2, expression of CIB1, STMN1 and Gankyrin was significantly elevated in tumour centre compared with both tumour margin and nontumourous liver tissues. In contrast, the level of 14-3-3 and ARIH1 was lower in the tumour centre versus nontumourous liver tissues. Notably, expression of CIB1 in tumour margin was markedly higher compared with nontumourous liver tissues, exhibiting a significant increase from nontumourous liver tissues to tumour centre (figure 2A).

2.5 *Immunostaining of CIB1 in HCC*

Among the identified proteins, CIB1 exhibited a high expression in cancer tissues, when compared with the corresponding normal tissues. CIB1 has attracted a lot of interest for its crucial role in functioning as a calcium-binding protein (White *et al.* 2006). Although CIB1 is considered as a regulator protein of calcium homeostasis under normal physiological conditions, the role of CIB1 in tumour growth is still controversial. Hence, in view of the fact that CIB1 is an important factor in the maintenance of normal cellular homeostasis and its enhanced expression contributes to oncogenic transformation, the interconnection between CIB1 and HCC became the subsequent focus of this study.

To further validate the elevation of CIB1 in clinical samples and with an aim to determine its role in HCC carcinogenesis, 100 groups of clinical samples were examined. The information of the clinical samples used in CIB1 immunostaining was listed in supplementary table 2. As shown in figure 3A, a significant increase tendency (TC *vs* TM $P<0.05$; TM *vs* NT $P<0.05$) was observed from nontumourous area to tumour centre in 72% (72/100) groups of samples. Further, stage-specific expression pattern of CIB1 was also analysed. In the 100 samples examined, 6 were in staging I, 38 were in staging II, 44 were in staging III, and 12 were in staging IV according to Surgical Pathologic Staging Criteria (6th edition, 2002). As shown in table 2, the level of CIB1 expression was significantly elevated in stage III and IV compared with stage I and II. To assess the correlation between overexpression of CIB1 and the survival rates, 100 patients were retrospectively studied. As shown in figure 3B, the 5-year survival rates were 44.6%, 18.1% and 17.9% for weak, moderate and strong immunoreactivity of CIB1, respectively. Together, our data demonstrated that CIB1 is overexpressed in HCC tissues, and is a potential prognostic factor for HCC.

2.6 *Suppression of CIB1 inhibit hepatoma cell proliferation*

In a pilot study, a siRNA targeting CIB1 was synthesized corresponding to previous report. Our data demonstrated that the expression of CIB1 was remarkably reduced when HepG2 cells were treated with CIB1-siRNA compared with the negative control control-siRNA (figure 4A).

To investigate the potential function of CIB1, the hepatoma HepG2 cell line was treated with CIB1-siRNA. As shown in figure 4B, CIB1 knockdown by CIB1-siRNA resulted in remarkable inhibition of liver cancer cell proliferation, which was demonstrated by 3H-thymidine incorporation assays. The data showed that cell proliferation was suppressed by CIB1-siRNA in a duration-dependent manner, and the proliferation ratio was decreased by 37.5% at 2.5 day and 41.2% at 3.5 day post-transfection, compared with the negative control.

3. Materials and methods

3.1 *Ethics statement*

The study was approved by the Institutional Ethics Committee of Zhujiang Hospital. All participants gave written informed consent prior to liver tissue sampling.

Table 1. Differentially identified proteins by

Spot no.	Accession no. (Swiss-Prot)	Protein name	Gene name	Theoretical MW (kDa)	Score	No. pep[a]	Sequence coverage (%)	Protein expression[b]	Gene ID
1	Q05CP7	Fatty acid binding protein 1, liver	FABP1	15,093	329	7	36	↓	2168
2	P16949	Stathmin 1	STMN1	17,303	621	9	33	↑	3925
3	P82912	28S ribosomal protein S11, mitochondrial	MRPS11	20,616	449	8	45	↓	64963
4	P37108	Signal recognition particle 14 kDa protein	SRP14	14,570	167	7	54	↑	6727
5	P23528	Cofilin 1	CFL1	18,502	198	8	40	↑	1072
6	P08708	40S ribosomal protein S17	RPS17	15,550	94	5	25	↑	6218
7	P63165	Small ubiquitin-related modifier 1	SUMO1	11,557	168	6	33	↑	7341
8	P06703	S100 calcium-binding protein A6	S100A6	10,180	224	9	50	↓	6277
9	Q99497	Protein DJ-1	PARK7	19,891	661	13	35	↑	11315
10	P18859	ATP synthase, H+ transporting, mitochondrial Fo complex, subunit F6	ATP5J	12,588	112	7	46	↑	522,
11	P26447	S100 calcium-binding protein A4	S100A4	22,783	660	10	50	↑	6275
12	A4D2P0	ras-related C3 botulinum toxin substrate 1	Rac1	23,467	93	4	38	↑	5879
13	Q99828	Calcium and integrin binding 1	CIB1	21,703	831	9	66	↑	10519
14	P24534	Eukaryotic translation elongation factor 1 beta 2	EEF1B2	24,764	153	4	25	↑	1933
15	O75832	Gankyrin	PSMD10	24,428	318	9	48	↑	5716
16	P12004	Proliferating cell nuclear antigen	PCNA	28,769	192	6	33	↑	5111
17	P08294	Superoxide dismutase 3, extracellular	SOD3	25,851	522	13	58	↑	6649
18	P30041	Peroxiredoxin-6	PRDX6	25,035	720	15	41	↑	9588
19	P61981	14-3-3 protein gamma	YWHAG	28,303	164	5	35	↑	7532
20	P32119	Peroxiredoxin 2	PRDX2	21,892	389	9	45	↑	7001
21	Q06830	Peroxiredoxin 1	PRDX1	22,110	269	5	25	↑	5052,
22	P32322	Pyrroline-5-carboxylate reductase 1	PYCR1	33,361	515	11	42	↓	5831
23	P14550	Alcohol dehydrogenase [NADP+]	AKR1A1	36,573	144	6	37	↑	10327
24	P42126	Dodecenoyl-CoA isomerase	DCI	32,816	216	9	36	↓	1632
25	Q96S97	Myeloid-associated differentiation marker	MYADM	35,274	99	4	50	↓	91663
26	O95684	FGFR1 oncogene partner	FGFR1OP	43,065	159	6	40	↑	11116,
27	P31947	14-3-3 protein sigma	SFN	27,774	629	13	51	↓	2810
28	P60174	Triosephosphate isomerase	TPI1	26,669	417	8	57	↑	7167
29	Q6NSF2	Ribosomal protein, large, P0	RPLP0	34,274	198	9	66	↑	6175
30	Q562R1	Beta-actin-like protein 2	ACTBL2	42,003	216	11	54	↑	345651
31	P00918	Carbonic anhydrase II	CA2	29,246	509	10	40	↓	760
32	P30084	Enoyl-CoA hydratase, mitochondrial	ECHS1	31,387	320	8	21	↓	1892
33	P04156	Major prion protein	PRNP	27,661	154	4	60	↑	5621
34	P12429	annexin A3	ANXA3	36,375	182	6	78	↑	306
35	P37837	Transaldolase	Taldo1	37,540	218	9	54	↑	6888
36	P11177	Pyruvate dehydrogenase E1 component subunit beta	PDHB	39,233	410	9	42	↑	5162,
37	P47756	Capping protein (actin filament) muscle Z-line, beta	CAPZB	31,350	261	6	32	↓	832
38	P00739	Haptoglobin-related protein	HPR	39,030	183	7	59	↑	3250
39	P00738	Haptoglobin	HP	45,205	114	5	45	↓	3240
40	P04075	Aldolase A, fructose-bisphosphate	ALDOA	39,420	165	4	25	↑	226,
41	P01009	Alpha-1-antitrypsin	SERPINA1	46,737	247	6	33	↑	5265

Table 1. (continued)

Spot no.	Accession no. (Swiss-Prot)	Protein name	Gene name	Theoretical MW (kDa)	Score	No. pep[a]	Sequence coverage (%)	Protein expression[b]	Gene ID
42	P06733	Enolase 1, (alpha)	ENO1	47,169	364	9	54	↑	2023
43	P02679	Fibrinogen gamma chain	FGG	51,512	198	7	61	↑	2266
44	Q03154	Aminoacylase 1	ACY1	45,885	508	10	36	↓	95
45	P05787	Keratin 8	KRT8	53,704	304	9	47	↓	3856
46	P08670	Vimentin	VIM	53,652	331	8	40	↑	7431
47	Q9BXM7	PTEN induced putative kinase 1	PINK1	62,769	203	6	66	↓	65018
48	Q9Y4X5	Ariadne homolog, ubiquitin- conjugating enzyme E2 binding protein, 1	ARIH1	64,118	778	13	58	↓	25820
49	Q6IB91	Phosphoenolpyruvate carboxykinase 2 (mitochondrial)	PCK2	70,697	190	3	48	↓	5106
50	P02768	Serum albumin	ALB	69,367	533	9	45	↑	213
51	O75908	Acetyl-CoA acetyltransferase 2	ACAT2	59,896	364	7	53	↓	39
52	P00367	Glutamate dehydrogenase 1, mitochondrial	GLUD1	61,398	408	10	46	↓	2746

a: Number of peptides identified.

b: ↑ indicates a protein that was upregulated in tumour centre, and ↓ indicates a protein that was downregulated in tumour centre.

3.2 *Tissue samples*

Clinical tissue samples were obtained from Zhujiang Hospital, Southern Medical University (Guangzhou, China). The specimens were diagnosed histologically after staining with H&E, and the surgical-pathologic stage was determined according to the TNM classification system of the International Union against Cancer. The donor HCC patients had not received any prior treatment before sampling. Information of the patients, such as age, sex, tumour size and HBV/HCV infection status, is listed in table 1. Tissue samples were immediately frozen in liquid nitrogen prior to immunoblotting or fixed in formalin prior to immunostaining.

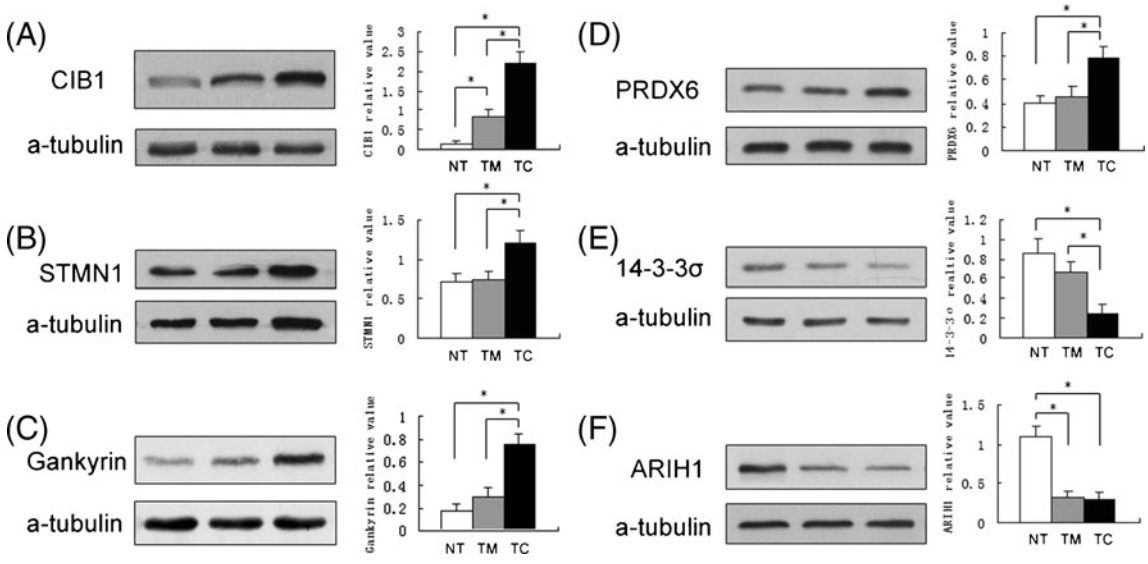

Figure 2. Validation of LC-MS/MS results by Western blotting using clinical samples. Representative Western blotting bands of CIB1 (**A**), STMN1 (**B**), Gankyrin (**C**), PRDX6 (**D**), 14-3-3 (**E**) and ARIH1 (**F**) were shown. Each data point represents the mean (*$P<0.05$ *vs* NT; $^{\#}P<0.05$ *vs* TM).

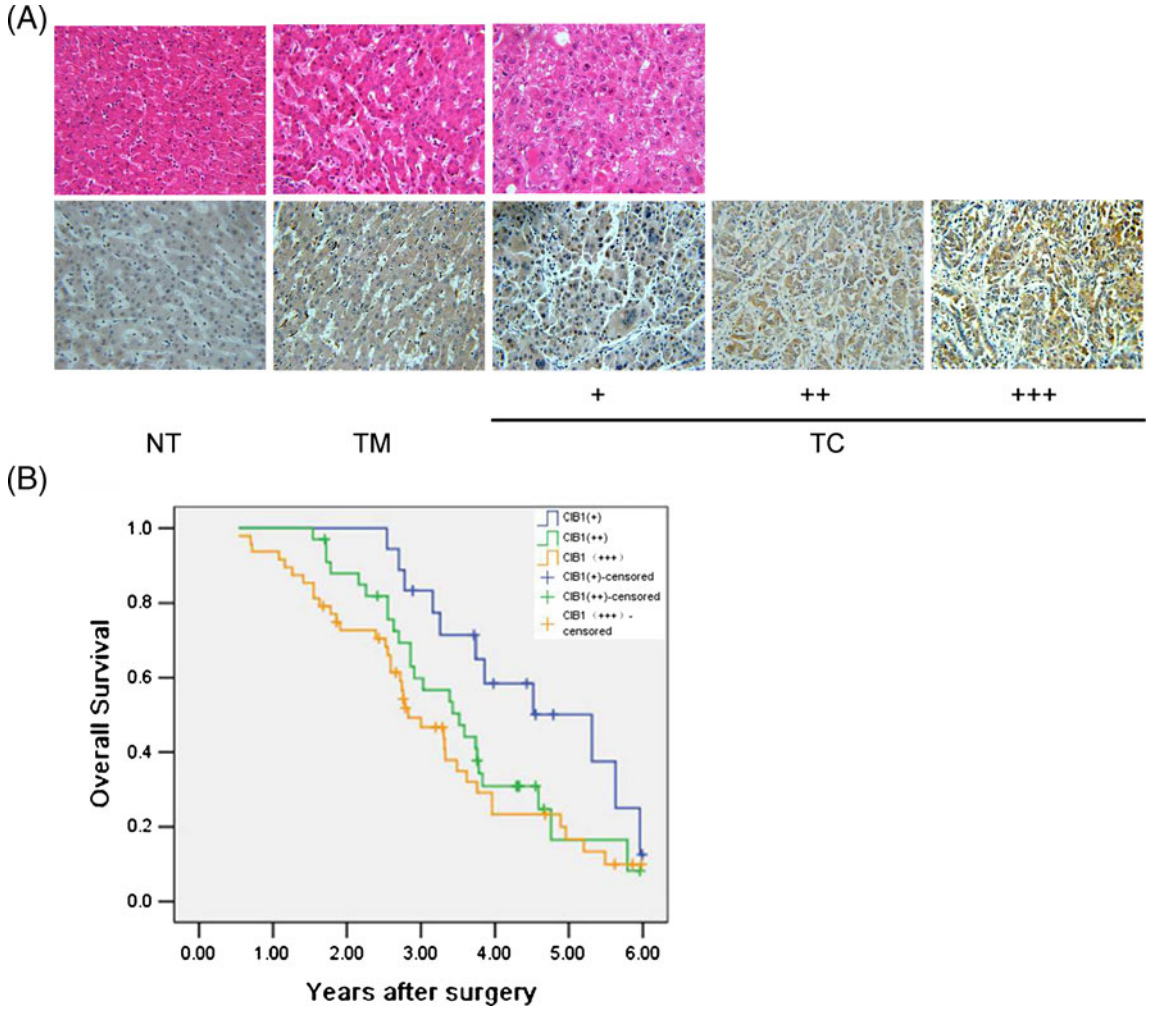

Figure 3. Representative H&E staining (upper panel) and immunostaining (bottom panel) of HCC tumour centre, tumour margin and nontumourous liver tissue (400×). Immunoreactivity of CIB1 in HCC tissues was evaluated by three stages, including weak (+), moderate (++) and strong (+++). (**A**) Kaplan–Meier survival curves showed the correlation between higher levels of CIB1 expression and lower survival rates ($P<0.05$).

Table 2. Stage-specific expression of CIB1 in HCC

	CIBI				
	+	++	+++	total	P^a
Stage					
I	3 (50%)	2 (33%)	1 (17%)	6	
II	8 (21%)	19 (50%)	11 (29%)	38	0.027[b]
III	6 (14%)	14 (32%)	24 (54%)	44	
IV	1 (9%)	4 (33%)	7 (58%)	12	
total	18	39	43	100	

[a] Kruskal–Wallis H test; [b] Statistically significant ($P<0.05$).

3.3 *2-DE*

100 mg of tissue sample was cut into pieces about 2 mm^3, homogenized in liquid nitrogen and lysed in 1 ml lysis buffer (7 M urea, 2 M thiourea, 4% CHAPS; BioRad, USA) containing protease inhibitor cocktail 8340 (Sigma, St Louis, MO, USA). Samples were then kept on ice and sonicated in 10 cycles each consisting of 10 s sonication followed by a 30 s break, and finally held for 30 min on ice with occasional vortex mixing. After centrifugation at 14000 rpm for 1 h at 4°C, proteins were precipitated with cold acetone at 20°C for 1 h and then dissolved with rehydration buffer (8 M urea, 2 M thiourea, 4% CHAPS, 100 mM DTT, and 2% ampholyte). Protein concentrations were determined using the DC protein assay kit (Bio-Rad). Individual sample concentrations were adjusted by dilution

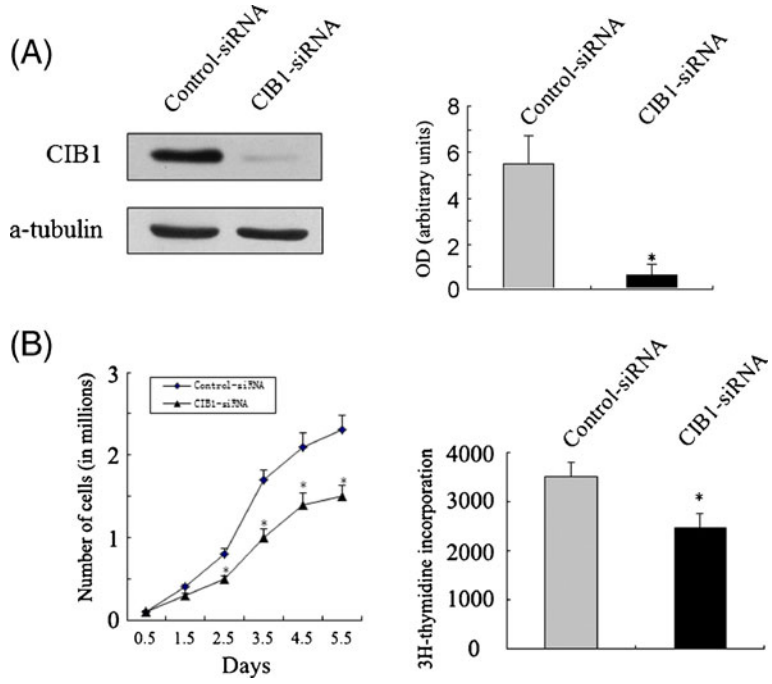

Figure 4. (**A**) HepG2 cells were transfected with CIB1-siRNA or the control siRNAs as described in Materials and methods. CIB1 expression was determined by Western blotting. (**B**) HepG2 cells were transfected with CIB1-siRNA or the control siRNAs. The level of cell proliferation was determined by 3H-thymidine incorporation.

in the same rehydration buffer. Samples were either applied immediately to Isoelectric Focusing (IEF) or stored at −80°C in aliquots prior to analysis. Protein samples (2.5 mg, 300 µl) were applied to IPG (immobilized pH gradient) strips (18 cm, pH 3–10, NL; Bio-Rad) using a passive rehydration method. After 12–16 h of rehydration, the strips were transferred to an IEF Cell (Bio-Rad). IEF was performed as follows: 250 V for 30 min, linear; 1000 V for 1 h, rapid; linear ramping to 10000 V for 5 h, and finally 10000 V for 6 h. Once IEF was completed, the strips were equilibrated in equilibration buffer (25 mM Tris–HCl, pH 8.8, 6 M urea, 20% glycerol, 2% SDS and 130 mM DTT) for 15 min, followed by the same buffer containing 200 mM iodoacetamide instead of DTT for another 15 min. The second dimension was performed using 12% SDS-PAGE at 30 mA constant current per gel. The gels were visualized using silver staining (Gorg *et al.* 1997; Rabilloud *et al.* 1997). For 2-DE analysis, each group of samples was run in triplicate to ensure the consistency of the data.

3.4 *Image analysis*

The images were scanned with a Bio-Rad GS-800 scanner (400–750 nm) and the differentially expressed proteins were identified using the PD-Quest 2D-analysis software (Bio-Rad, USA). The quantity of each spot in a gel was normalized as a percentage of the total quantity in the map according to its OD value.

3.5 *Tryptic in-gel digestion*

In-gel digestion of proteins was carried out using mass spectrometry grade trypsin gold (Promega, Madison, WI, USA) according to the manufacturer's instructions. Briefly, spots were cut out of the gel (1–2 mm diameter) using a razor blade, and de-stained twice with 100 mM NH_4HCO_3/50% acetonitrile (ACN) at 37°C for 45 min in each treatment. After dehydration with 100% ACN and drying, the gels were pre-incubated in 10–20 µl trypsin solution (10 ng/µl) for 1 h. Then, adequate digestion buffer (40 mM NH_4HCO_3/10% ACN) was added to cover the gels, which were incubated overnight at 37°C (12–14 h). Tryptic digests were extracted using MilliQ water, followed by double extraction with 50% ACN/5% trifluoroacetic acid (TFA) for 1 h each time. The combined extracts were dried in a speed-VAC concentrator (Thermal, USA) at 4°C. The samples were then subjected to mass spectrometry.

3.6 *ESI-Q-TOF*

Mass spectra were acquired using a Q-TOF mass spectrometer (Micromass, Manchester, UK) fitted with an ESI source (Waters). Tryptic digests were dissolved in 18 µl 50% ACN. MS/MS was performed in a data-dependent mode in which the top 10 most abundant ions for each MS scan were selected for MS/MS analysis. Trypsin autolysis products

and keratin derived precursor ions were automatically excluded. Protein identification was accomplished using MassLynx software (Micromass) and MASCOT 2.1 (Matrixscience) search engine against the SwissProt 57.8 database. Database searches were carried out using the following parameters: database, Swiss-Prot; taxonomy, *Homo sapiens*; enzyme, trypsin; and allowance of one missed cleavage. The peptide and fragment mass tolerance were set at 0.1 and 0.05 Da, respectively. Protein scores are derived from ions scores as a non-probabilistic basis for ranking protein hits. Individual ions scores>38 indicate identity or extensive homology ($P<0.05$).

3.7 *Western blotting*

Proteins were extracted in RIPA buffer (50 mM Tris-base, 1.0 mM EDTA, 150 mM NaCl, 0.1% SDS, 1% TritonX-100, 1% Sodium deoxycholate, 1 mM PMSF) and quantified by the DC protein assay kit (Bio-Rad). Samples were separated by 12% SDS-PAGE and transferred to PVDF membranes (Amersham Biosciences). The membranes were blocked overnight with PBS containing 0.1% Tween 20 in 5% skimmed milk at 4°C, and subsequently probed by the primary antibodies: mouse-anti-CIB1 (diluted 1:1000 Santa Cruz), mouse-anti-STMN1 (diluted 1:1000 Santa Cruz), rabbit-anti-Gankyrin (diluted 1:1000; Santa Cruz), rabbit-anti-PRDX6 (diluted 1:1000 abcam), mouse-anti-14-3-3σ (diluted 1:1000 Santa Cruz), mouse-anti-ARIH1 (diluted 1:1000 Santa Cruz), rabbit-anti-α-tubulin (diluted 1:1000 Santa Cruz). Blots were incubated with the respective primary antibodies for 2 h at room temperature. After washing 3 times in TBST, the blots were incubated with secondary antibody (diluted 1:10000 Santa Cruz) conjugated to horseradish peroxidase for 2 h at room temperature. Blots were visualized by enhanced chemiluminescence reagents (Amersham Pharmacia Biotech, Piscataway, USA). α-tubulin was used as an internal control.

3.8 *Immunohistochemistry*

Immunohistochemistry was performed using the Dako Envisions Systems (Dako Cytomation GmbH, Hamburg, Germany). Consecutive paraffin-wax-embedded tissue sections (3–5 μm) were de-waxed and re-hydrated. Antigen retrieval was performed by pretreatment of the slides in citrate buffer (pH 6.0) in a microwave oven for 12 min. Thereafter, slides were cooled to room temperature in de-ionised water for 5 min. Endogenous peroxidase activity was quenched by incubating the slides in methanol containing 0.6% hydrogen peroxide, followed by washing in deionised water for 3 min, after which the sections were incubated for 1 h at room temperature with normal goat serum, and subsequently incubated at 4°C overnight with the primary antibodies: mouse-anti-CIB1 (diluted 1:400 Santa Cruz). Next, the sections were rinsed with washing buffer (TBS with 0.1% bovine serum albumin) and incubated with horseradish peroxidase linked goat anti-rabbit antibodies, followed by reaction with diaminobenzidine and counterstaining with Mayer's haematoxylin. Immunostaining was detected using DAB substrate solution (Dako Cytomation GmbH, Hamburg, Germany) according to the manufacturer's instructions.

The intensity of CIB1 staining was evaluated in each sample and graded from 0 to 4 (no staining is scored as 0, 1%–10% of cells stained scored as 1, 11%–50% as 2, 51%–80% as 3, and 81%–100% as 4) and 0–3 (0 is defined as negative, 1 as weak, 2 as moderated, and 3 as strong), respectively. The raw data were calculated into the immunohistochemical score (IHS) by multiplying the quantity and intensity scores. An IHS score of 9–12 was considered as strong immunoreactivity (+++), 5–8 as moderate (++), 1–4 as weak (+), and 0 as negative (Liu *et al*. 2010).

3.9 *siRNA*

Double-strand siRNA oligonucleotide targeting CIB1 and control siRNA were purchased from Santa Cruz. Usage and storage of siRNA was according to the manufacturer's recommendation.

3.10 *Cell culture and transfection*

The human hepatoma HepG2 cells cell line (ATCC, Manassas, VA) was maintained in Dulbecco's modified Eagles medium (DMEM) medium (GBICO) with 10% FBS. The Lipofectamine 2000 (Invitrogen) and siRNA were diluted in antibiotics-free medium, respectively, and then combined at a ratio of 2.5:1. The combinations were transfected into the cells in the indicated concentrations according to the manufacturer's recommendation.

3.11 *Cell proliferation assay*

CIB1-siRNA- and control-siRNA-transfected cells were seeded (1×10^4 cells/well) in triplicate onto 24-well plates pre-coated with 30 μg/ml of collagen type I (Sigma). At two-day intervals, cells from triplicate wells were counted. In a separate set of experiments the cells were incubated with 3H-thymidine (0.2 μCi; Amersham) and the extent of 3H-thymidine incorporation was determined using scintillation counter.

3.12 *Data analysis and statistics*

Comparisons between two groups were performed by Student's *t*-test. Statistical significance was defined as

$P<0.05$. Comparisons between multiple groups were performed by Kruskal–Wallis H test. Statistical significance was defined as $P<0.05$.

4. Discussion

HCC, among the most common malignancies worldwide, remains a major threat to public health, and there is an urgent need to identify novel biomarkers for diagnosis, prognosis and targets for anti-cancer treatment (Farazi and DePinho 2006). In this study, 2-DE-based proteomics approach was employed to profile the altered expressed proteins among HCC tumour centre, tumour margin and nontumourous liver tissues, leading to identification of 52 distinct proteins with altered expression, which were associated with diverse biological function. Some of these altered proteins, such as fatty acid binding protein 1, Cofilin 1, S100 calcium-binding protein A4, Protein DJ-1, annexin A3 and enolase 1, have been evidenced to be associated with HCC in previous studies but without clinical validation and functional analyses (Feng *et al.* 2006; Minagawa *et al.* 2008; Wang *et al.* 2009). However, most of these altered proteins have been found to be involved in multiple cellular pathways related to carcinogenesis (e.g. apoptosis, differentiation, proliferation, migration and invasion). Clearly, there is a need for further studies to elucidate the precise functional roles of these individual proteins in the cellular signalling pathway as well as in the initiation and development of cancers.

Among the altered proteins, CIB1 was originally identified as a small, ubiquitous protein with calcium-binding activity, and as such it has attracted increasing attention (White *et al.* 2006). CIB1 consists of four helix-loop-helix 'EF-hand' Ca2-binding motifs (EF-I to EF-IV), as well as a myristoylated N-terminal extension, and a short C-terminal extension which folds back on the protein and increases target-binding specificity (Gentry *et al.* 2005). In addition, CIB1 was also evidenced as binding partner for the cytoplasmic tail of the platelet integrinαIIβ (Yuan *et al.* 2006). Recently, more CIB1-binding proteins were identified, including DNA-dependent protein kinase, the polo-like kinases Fnk and Snk, Rac3, Pax3, and presenilin 2, and CIB1 has been shown to modify the function of some of these proteins (Gentry *et al.* 2005).

The full spectrums of interactions that link CIB1 with tumours have not yet to be fully illustrated. However, some pioneering work focused on the role of CIB1 in tumour angiogenesis has been undertaken using CIB1-knockout mice. It is reported that endothelial cells from CIB1-knockout mice showed an attenuated responses to angiogenic growth factors such as VEGF and FGF-2, which result in decreased expression of the zinc-requiring matrix-degrading proteinase MMP-2, leading to an impaired angiogenesis in melanoma xenograft model. Further, loss of CIB1 in endothelial cells disturbed various pro- and anti-angiogenic signallings, including PAK1 and ERK1/2 (Zayed *et al.* 2010). Recently, investigations regarding the interactions of CIB1 with regulatory factors in signalling transduction pathways have shed light on the roles of CIB1 in cancer cell adaptation to apoptotic stress. It is reported that CIB1 renders breast cancer MCF7 cells to reactive oxygen species (ROS) and by TNF-α-induced apoptosis by physically binding to ASK1, leading to inhibition of the ASK1-JNK and ASK1-p38 signalling (Yoon *et al.* 2009). In further support of this, a recent work showed that CIB1 inhibited Plk3-mediated cell cycle arrest in breast cancer cells by constitutively interacting with Plk3, and this inhibition activity is Ca^{2+}-dependent (Kostyak and Naik 2011). Thus, the marked impact of CIB11 on cell proliferation may be related to the wide variety of signalling complexes to which CIB1 binds in a cell-type-specific manner. Therefore, HCC appears to be a good model for further study on the cell-type-specific involvement of CIB1 in human tumours.

To the best of our knowledge, this is the first report regarding the association of CIB1 with HCC based on the proteomic analysis. The intensity of both immunoblotting and immunostaining among nontumourous liver tissues, tumour margin and HCC tumour centre has revealed a remarkable increased tendency. The present data suggests that CIB1 may be used as a potential biomarker in the prediction of prognosis for HCC patients. More importantly, our data demonstrated a dramatic elevation of CIB1 in HCC tumour margin compared with nontumourous liver, suggesting the notion that overexpression of CIB1 may occurs in the initial steps during HCC carcinogenesis.

Recently, RNA interference has been proposed as one of the most novel potential gene therapy strategies (Ryther *et al.* 2005). The observed significant difference in proliferation between HepG2 cells treated with CIB1-siRNA and control-siRNA, strongly suggested that CIB1 could be considered as a potential therapeutic target against HCC. Further experiments will be conducted to determine whether silencing CIB1 expression has the same inhibitory effects on HCC tumour growth *in vivo*, through the establishment of a human HCC xenograft-nude mouse model.

Acknowledgements

This work was supported by the National 863 High-Tech Foundation (Grant 2006AA02A141). The funders had no role in study design, data collection and analysis, decision to publish, or preparation of the manuscript. TJ, ZH and HF conceived and designed the experiments. ZH, HF, YX, LZ, ZH, ZJ, WY, HY, ZJ, SL and HG performed the experiments. ZH and HF analysed the data. ZH and HF contributed reagents/materials/analysis tools and wrote the paper.

References

Cho WC 2007 Contribution of oncoproteomics to cancer biomarker discovery. *Mol Cancer* **6** 25

Comunale MA, Lowman M, Long RE, Krakover J, Philip R, Seeholzer S, Evans AA, Hann HW, Block TM and Mehta AS 2006 Proteomic analysis of serum associated fucosylated glycoproteins in the development of primary hepatocellular carcinoma. *J. Proteome Res.* **5** 308–315

El-Serag HB and Rudolph KL 2007 Hepatocellular carcinoma: epidemiology and molecular carcinogenesis. *Gastroenterology* **132** 2557–2576

Farazi PA and DePinho RA 2006 Hepatocellular carcinoma pathogenesis: from genes to environment. *Nat. Rev. Cancer* **6** 674–687

Feng JT, Shang S and Beretta L 2006 Proteomics for the early detection and treatment of hepatocellular carcinoma. *Oncogene* **25** 3810–3817

Gentry HR, Singer AU, Betts L, Yang C, Ferrara JD, Sondek J and Parise LV 2005 Structural and biochemical characterization of CIB1 delineates a new family of EF-hand-containing proteins. *J. Biol. Chem.* **280** 8407–8415

Gorg A, Postel W, Weser J, Gunther S, Strahler JR, Hanash SM and Somerlot L 1987 Elimination of point straking on silver-stained two-dimensional gels by addition of iodoacetamide to the equilibration buffer. *Electrophoresis* **8** 122–124

Hwang LH 2006 Gene therapy strategies for hepatocellular carcinoma. *J. Biomed. Sci.* **13** 453–468

Kostyak JC and Naik UP 2011 Calcium- and integrin-binding protein 1 regulates endomitosis and its interaction with polo-like kinase 3 is enhanced in endomitotic dami cells. *PLoS One* **6** e14513

Liu X, Cheng Y, Sheng W, Lu H, Xu Y, Long Z, Zhu H and Wang Y 2010 Clinicopathologic features and prognostic factors in alpha-fetoprotein-producing gastric cancers: analysis of 104 cases. *J. Surg. Oncol.* **102** 249–255

Maass T, Sfakianakis I, Staib F, Krupp M, Galle PR and Teufel A 2010 Microarray-based gene expression analysis of hepatocellular carcinoma. *Curr. Genomics* **11** 261–268

Minagawa H, Honda M, Miyazaki K, Tabuse Y, Teramoto R, Yamashita T, Nishino R, Takatori H, Ueda T, Kamijo K, *et al.* 2008 Comparative proteomic and transcriptomic profiling of the human hepatocellular carcinoma. *Biochem. Biophys. Res. Commun.* **366** 186–192

Petricoin EF, Zoon KC, Kohn EC, Barrett JC and Liotta LA 2002 Clinical proteomics: translating benchside promise into bedside reality. *Nat. Rev. Drug Discov.* **1** 683–695

Rabilloud T, Adessi C, Giraudel A and Lunardi J 1997 Improvement of the solubilization of proteins in two-dimensional electrophoresis with immobilized pH gradients. *Electrophoresis* **18** 307–316

Raza SA, Clifford GM and Franceschi S 2007 Worldwide variation in the relative importance of hepatitis B and hepatitis C viruses in hepatocellular carcinoma: a systematic review. *Br. J. Cancer.* **96** 1127–134

Ryther RC, Flynt AS, Phillips JA 3rd and Patton JG 2005 siRNA therapeutics: big potential from small RNAs. *Gene Ther.* **12** 5–11

Sun W, Xing B, Sun Y, Du X, Lu M, Hao C, Lu Z, Mi W, Wu S, Wei H, *et al.* 2007 Proteome analysis of hepatocellular carcinoma by two-dimensional difference gel electrophoresis: novel protein markers in hepatocellular carcinoma tissues. *Mol. Cell Proteomic.* **6** 1798–1808

Tseng PL, Tai MH, Huang CC, Wang CC, Lin JW, Hung CH, Chen CH, Wang JH, Lu SN, Lee CM, *et al.* 2008 Over-expression of VEGF is associated with positive p53 immunostaining in hepatocellular carcinoma (HCC) and adverse outcome of HCC patients. *J. Surg. Oncol.* **98** 349–357

Wang F, Kaur S, Cavin LG and Arsura M 2008 Nuclear-factor-kappaB (NF-kappaB) and radical oxygen species play contrary roles in transforming growth factor-beta1 (TGF-beta1)-induced apoptosis in hepatocellular carcinoma (HCC) cells. *Biochem. Biophys. Res. Commun.* **377** 1107–1112

Wang X, Chen Y, Han QB, Chan CY, Wang H, Liu Z, Cheng CH, Yew DT, Lin MC, He ML, *et al.* 2009 Proteomic identification of molecular targets of gambogic acid: role of stathmin in hepatocellular carcinoma. *Proteomics* **9** 242–253

White C, Yang J, Monteiro MJ and Foskett JK 2006 CIB1, a ubiquitously expressed Ca2+—binding protein ligand of the InsP3 receptor Ca2+ release channel. *J. Biol. Chem.* **281** 20825–20833

Wulfkuhle JD, Liotta LA and Petricoin EF 2003 Proteomic applications for the early detection of cancer. *Nat. Rev. Cancer* **3** 267–275

Yoon KW, Cho JH, Lee JK, Kang YH, Chae JS, Kim YM, Kim J, Kim EK, Kim SE, Baik JH, *et al.* 2009 CIB1 functions as a Ca (2+)-sensitive modulator of stress-induced signaling by targeting ASK1. *Proc. Natl. Acad. Sci. USA* **106** 17389–17394

Yuan W, Leisner TM, McFadden AW, Wang Z, Larson MK, Clark S, Boudignon-Proudhon C, Lam SC, Parise LV, *et al.* 2006 CIB1 is an endogenous inhibitor of agonist-induced integrin alphaIIbbeta3 activation. *J. Cell Biol.* **172** 169–175

Zayed MA, Yuan W, Chalothorn D, Faber JE and Parise LV 2010 Tumor growth and angiogenesis is impaired in CIB1 knockout mice. *J. Angiogenes Res.* **2** 17

MS received 28 February 2011; accepted 30 May 2011

*e*Publication: 16 August 2011

Corresponding editor: RITA MULHERKAR